Article

Chinese Science Bulletin

Mechanical Engineering

April 2012 Vol.57 No.10: 1209–1216
doi: 10.1007/s11434-012-5005-6

Multimodal swimming control of a robotic fish with pectoral fins using a CPG network

WANG Ming[1,2], YU JunZhi[2*], TAN Min[2] & ZHANG JianWei[3]

[1] *School of Information and Electrical Engineering, Shandong Jianzhu University, Jinan 250101, China;*
[2] *State Key Laboratory of Management and Control for Complex Systems, Institute of Automation, Chinese Academy of Sciences, Beijing 100190, China;*
[3] *Department of Informatics, University of Hamburg, Hamburg, D-22527, Germany*

Received June 11, 2011; accepted December 29, 2011

The neural-based approaches inspired by biological neural mechanisms of locomotion are becoming increasingly popular in robot control. This paper investigates a systematic method to formulate a Central Pattern Generator (CPG) based control model for multimodal swimming of a multi-articulated robotic fish with flexible pectoral fins. A CPG network is created to yield diverse swimming in three dimensions by coupling a set of nonlinear neural oscillators using nearest-neighbor interactions. In particular, a sensitivity analysis of characteristic parameters and a stability proof of the CPG network are given. Through the coordinated control of the joint CPG, caudal fin CPG, and pectoral fin CPG, a diversity of swimming modes are defined and successfully implemented. The latest results obtained demonstrate the effectiveness of the proposed method. It is also confirmed that the CPG-based swimming control exhibits better dynamic invariability in preserving rhythm than the conventional body wave method.

bio-inspired control, central pattern generator (CPG), neural network, robotic fish, swimming control

Citation: Wang M, Yu J Z, Tan M, et al. Multimodal swimming control of a robotic fish with pectoral fins using a CPG network. Chin Sci Bull, 2012, 57: 1209–1216, doi: 10.1007/s11434-012-5005-6

Robotic fish, inspired by fish in nature, have received increasing attention in recent years because of potential aquatic-related applications such as exploration, surveillance, transportation, and mobile sensing [1–7]. Many scientists and engineers have carried out studies on robotic fish, focusing not only on the hydrodynamics mechanism and bio-inspired practice of fishlike swimming, but also on motion planning, control, and optimization of the fishlike robots [2]. The current swimming control methods, from the perspective of cybernetics, tend to fall into two primary categories: bio-inspired and non-bio-inspired (conventional). The former is nourished by an abundance of biological knowledge of fish or other animals, while the latter relates to deriving control laws from a combined analysis of multi-body dynamics and kinematics.

To achieve flexible swimming control, conventional locomotion control usually seeks to calculate propulsive forces and to determine the accompanying movements. Once the dynamic equation attached to each propulsive component has been identified via synthesizing all involved dynamic equations, the control laws can be obtained in terms of the resultant forces and kinematic parameters of the moving joints. As a rule, oscillatory frequency, amplitude, as well as phase difference between adjacent joints are usually extracted as the locomotion-related characteristics significantly affecting swimming performance. Many robotic fishes are controlled in such a manner, for example, the well-known Robotuna [8], the pectoral-fin-driven robotic Blackbass [9], and the lifelike Mitsubishi robotic fish [10]. However, two issues arise in determining appropriate swimming parameters: (1) the difficulty in accurately modeling the hydrodynamic interaction between the oscillating fish body and its surrounding fluid, and (2) an infinity of possible solutions in the hyper-redundant planar kinematic

*Corresponding author (email: junzhi.yu@ia.ac.cn)

chain [10]. Some researchers have therefore, resorted to alternative control methods, such as bio-inspired control. Inspired by the lamprey whose undulatory motions are governed by central pattern generators (CPGs), more recent studies employ CPGs to generate fishlike swimming in the context of neural-based control [11].

The CPGs are networks of nonlinear oscillating neurons able to produce rhythmic patterns without control inputs from high levels and also to be automatically synchronized [12]. There have been many research studies on replicating fishlike swimming [12,13] and snake-like serpentine motions [14–16] via artificial CPGs in past decades. For instance, Cohen et al. [17] presented a simplified mathematical model to explain the intersegmental coordination of neural networks in the isolated spinal cord of the lamprey, while Crespi et al. [18] extended a lamprey-like CPG-based model to control the locomotion of a fish robot on land and in water. Zhao et al. [19] and Zhang et al. [20] utilized a chain of nonlinear oscillators to construct a CPG for steady planar swimming. Besides rhythmic motion, CPGs have been extended to cover non-rhythmic (discrete) motion [21]. However, only a few studies have been conducted on the systematic design and control of rhythmic and discrete swimming, i.e., multimodal swimming, under a framework of CPG control.

The objective of this paper is to generate and control bio-inspired multimodal swimming via a well-formulated CPG network model. Compared with our previous work on rhythmic swimming excited by nonlinear oscillators [19, 22], we include three major improvements. (1) The parameter sensitivity analysis and stability proof of the CPG network are given. (2) The multimodal swimming gaits are successfully realized by coordinated movements of the caudal fin (CF), body-caudal fin (BCF), and pectoral fins (PF). (3) A comparison with the conventional body wave method is presented, thus demonstrating good applicability of CPG-based control in a dynamically changing environment.

1 Overview of robotic fish prototype

To approximate a given smooth, spatial- and time-varying body wave observed in real fish, as described by Yu et al. [3,22], the relative link lengths are optimized and further applied to calculate discrete swimming data. Figure 1 depicts an improved, radio-controlled, four-link, self-propelled robotic fish prototype. Mechanically the robot consists of a head and anterior body, a multi-articulated posterior body, a caudal fin, as well as a pair of pectoral fins. The shell of the head and anterior body is made of fiber reinforced plastic, offering a hollow and watertight space housing electronics, sensors, control components, batteries, and balancing weight. The posterior part comprises four servomotors connected in series with metal links, whose outside is wrapped by a compliant, crinkled rubber tube functioning as the fish skin. With regard to the accessory fins, a crescent-shaped caudal fin is connected to the last link, while a pair of wing-like pectoral fins is symmetrically placed at the rear lower position of the head. Notice that each pectoral fin, capable of 0–360° rotation via a set of custom-built gears, can be controlled independently or synchronously. The fish robot is 600 mm in length and weighs 3.22 kg. Both pectoral fins have the same dimensions, that is, 120 mm in length, 80 mm in width, and 5 mm in height.

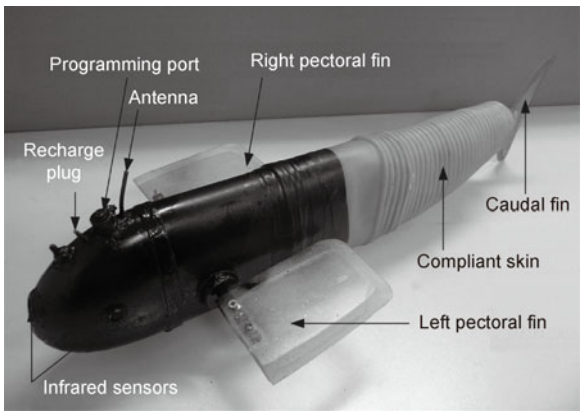

Figure 1 The multimodal swimming-oriented robotic prototype.

Our robotic fish is propelled by the flexible posterior body and oscillating tail and/or by the artificial pectoral fins. With three infrared sensors detecting obstacles at the front, left and right sides of the fish head and one pressure sensor detecting the depth, the robot is able to swim autonomously. Available swimming modes based on trial and error involve forward/backward swimming, turning, pitching, and combined maneuvers. Specifically, for instance, the robotic fish can perform forward swimming via BCF mode, via PF mode, via CF mode, or via a combination of these. Table 1 summarizes the relation between swimming modes and the control surfaces involved.

2 Bio-inspired CPG network

In this section, we mainly present the formulation of the CPG network, describing its stability proof, coupling scheme, as well as generation of multimodal swimming.

2.1 Analysis of neural oscillator model

At present, there are three popular types of neural oscillators

Table 1 Relation between swimming modes and control surfaces

Swimming modes	Control surfaces involved			
Forward swimming	BCF	PF	CF	BCF+PF, CF+PF
Backward swimming		PF		BCF+PF
Turning	BCF	PF		BCF+PF
Pitching		PF		BCF+PF

for multi-articulated movement in robotics: the Matsuoka (recurrent) neural oscillator, the phase oscillator, and the Van der Pol neural oscillator [23]. In particular, the phase oscillator model is usually utilized in fishlike swimming. For example, Cohen et al. [17] proposed a relatively simple limit cycle model with only a single dependent variable, the phase $\theta(t)$. To model the CPG of a multilink robotic fish, a novel nonlinear neural oscillator model with explicit control variables is created as follows:

$$\begin{cases} \dot{p} = \omega(p-q) - \mu p(p^2+q^2), \\ \dot{q} = \omega(p+q) - \mu q(p^2+q^2), \end{cases} \tag{1}$$

where state variables p and q denote the membrane potential and adjustment potential of the CPG oscillator, respectively; ω is a positive parameter influencing the oscillatory frequency and amplitude of the system; and μ is a coefficient that relates merely to the oscillatory amplitude. The combined regulation of the oscillatory frequency and amplitude accords with actual fish swimming, thereby adequately facilitating the engineering realization of swimming control.

Mathematically, it can be proved that, when $\omega > 0$ and $\mu > 0$, the system in eq. (1) has an asymptotic stable limit cycle whose asymptotic amplitude is $\sqrt{\omega/\mu}$ and angular frequency is ω. Let $p = r\cos\theta$ and $q = r\sin\theta$; then, for any initial value (r_0, θ_0), the solution of eq. (1) can be derived as

$$\varphi_t(r,\theta) = \left(\sqrt{\omega/\mu} \cdot (1-(1-\mu^{-1}r_0^{-2}\omega)\mathrm{e}^{-2\omega t})^{-\frac{1}{2}}, \omega t + \theta_0 \right). \tag{2}$$

For the purpose of analyzing the impact of parameters ω and μ on state variables p and q, the amplitude relative error e_r is defined as

$$e_r = \frac{\left| r(t) - \lim\limits_{t\to\infty} r(t) \right|}{\lim\limits_{t\to\infty} r(t)} = \left| (1-(1-\mu^{-1}\omega)e^{-2\omega t})^{-\frac{1}{2}} - 1 \right|. \tag{3}$$

Since the initial value r_0 has some bearing on $r(t)$, for simplicity, let $r_0 = 1$. Thus, there are two variables ω and μ in eq. (3), where μ is assumed to be a positive constant. For $\mu = 0.1$, the impact of parameter ω is plotted in Figure 2. As can be seen, the relative error e_r converges to zero more rapidly with an increasing ω. At the same time, the influence of parameter μ is plotted in Figure 3, where $\omega = 10$. Similar to the trend displayed in Figure 2, the relative error e_r converges to zero more rapidly with an increasing μ. Specially, when $\mu = \omega = 10$, $e_r = 0$. In this situation, the oscillatory amplitude $\lim\limits_{t\to\infty} r(t) = 1$. Considering that $\lim\limits_{t\to\infty} r(t) = 1$ is too small for robotic fish control, μ should deliberately be chosen at a value less than ω, that is, $\mu<10$.

2.2 Analysis of CPG network model

By coupling a set of neural oscillators defined by eq. (1), a

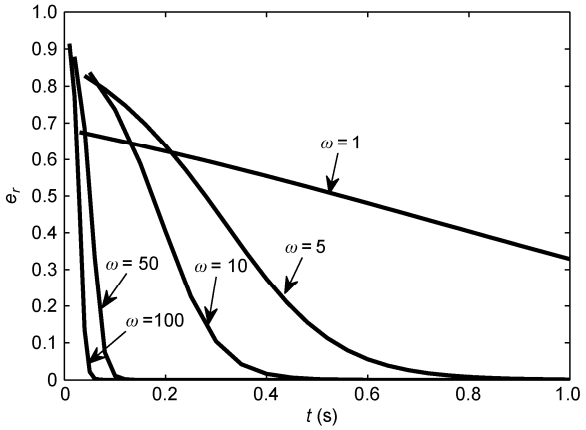

Figure 2 Impact of ω on the output quantity q_i.

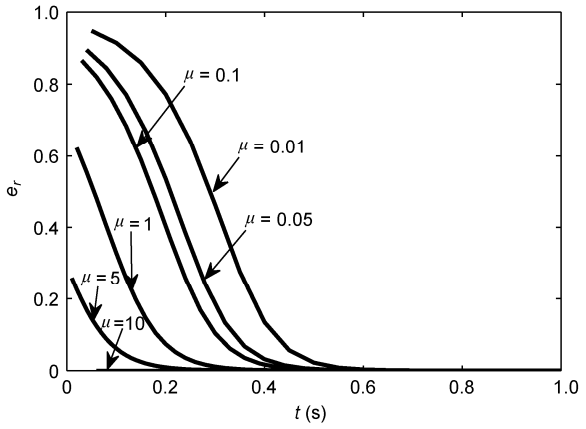

Figure 3 Impact of μ_i on the output quantity q_i.

CPG network model can mathematically be formulated as:

$$\begin{cases} \dot{p}_i = \omega(p_i - q_i) - \mu_i p_i(p_i^2+q_i^2) + \sum\limits_{j=1}^{n} a_{ij} q_j, \\ \dot{q}_i = \omega(p_i + q_i) - \mu_i q_i(p_i^2+q_i^2), \end{cases} \tag{4}$$

where $i = 1, \cdots, n$, and n represents the total number of CPG units in the network. The coupling relationship of the i-th CPG with other CPG units in the network is expressed as $\sum_{j=1}^{n} a_{ij} q_j$. Note that $\sum_{j=1}^{n} a_{ij} q_j > 0$ is defined so that the effects from other CPG units will excite the activity of the i-th one; whereas $\sum_{j=1}^{n} a_{ij} q_j < 0$ is defined so that other CPG units will inhibit the activity of the i-th one.

Theorem 1: The system defined by eq. (4) has a unique solution for any initial condition (p_{i0}, q_{i0}).

Proof: The existence and uniqueness of a solution can be guaranteed if the system defined by eq. (4) is of the Lipschitz type.

Assume that $|t-t'| < \sigma$, $|p_i - p_i'| < \sigma_1$, $|q_i - q_i'| < \sigma_2$, where σ, σ_1, and σ_2 are positive constants. Then, we rewrite the differential equations in eq. (4) in the form:

$$\begin{cases} f(t,p_i)=\omega(p_i-q_i)-\mu_i p_i(p_i^2+q_i^2)+\sum_{j=1}^{n}a_{ij}q_j, \\ g(t,q_i)=\omega(p_i+q_i)-\mu_i q_i(p_i^2+q_i^2). \end{cases} \tag{5}$$

Then, it follows that

$$\begin{aligned} |g(t,q_i)-g(t',q_i')| = & \ |\omega(p_i-p_i')+\omega(q_i-q_i') \\ & +\mu_i[q_i'(p_i'^2+q_i'^2)-q_i(p_i^2+q_i^2)]|. \end{aligned} \tag{6}$$

To further obtain the condition satisfying the Lipschitz-type function, the differential mean value theorem is employed. According to the mean value theorem, $f:[a,b]\to R$ is a continuous function on the closed interval [*a*,*b*] and differentiable on the open interval (*a*,*b*), where $a<b$. Then, there exists some $c\in(a,b)$ matching $f(b)$–$f(a)=(b-a)\cdot f'(c)$.

Suppose that $q_i<q_i'$, $\max(|q_i'|,|q_i|)\leqslant M$, $\max(|p_i'|,|p_i|)\leqslant N$, where M and N are positive constants. If $h(q)=q^3$, obviously, function $h(q)$ meets the requirements of the mean value theorem in $[q,q']$. Then there exists some $c\in(q,q')$ that satisfies the following relations:

$$\begin{aligned} h(q_i)-h(q_i')=q_i^3-q_i'^3=(q_i-q_i')h'(c)=3c^2(q_i-q_i') \\ \leqslant 3M^2|q_i-q_i'| \end{aligned} \tag{7}$$

and

$$q_i'p_i'^2-q_ip_i^2\leqslant 2MN^2. \tag{8}$$

Combining eqs. (6)–(8) yields

$$\begin{aligned} & |g(t,q_i)-g(t',q_i')| \\ & =\left|\omega(p_i-p_i')+\omega(q_i-q_i')+\mu_i[q_i'(p_i'^2+q_i'^2)-q_i(p_i^2+q_i^2)]\right| \\ & \leqslant\left|\frac{\omega(\sigma_1+\sigma_2)}{\sigma_2}\right||q_i-q_i'|+|3\mu_iM^2||q_i-q_i'|+\left|\frac{2\mu_iMN^2}{\sigma_2}\right||q_i-q_i'| \\ & =\left(\left|\frac{\omega(\sigma_1+\sigma_2)}{\sigma_2}\right|+|3\mu_iM^2|+\left|\frac{2\mu_iMN^2}{\sigma_2}\right|\right)|q_i-q_i'|=L_1|q_i-q_i'|, \end{aligned} \tag{9}$$

where $L_1=\left|\frac{\omega(\sigma_1+\sigma_2)}{\sigma_2}\right|+|3\mu_iM^2|+\left|\frac{2\mu_iMN^2}{\sigma_2}\right|$.

Then, it follows that

$$\begin{aligned} f(t,p_i)-f(t',p_i')=\omega(p_i-p_i')+\omega(q_i-q_i')+\mu_ip_i'(p_i'^2+q_i'^2) \\ -\mu_ip_i(p_i^2+q_i^2)+\sum_{j=1}^{n}a_{ij}(q_j-q_j'). \end{aligned} \tag{10}$$

Let $\max_{1\leqslant i\leqslant n,1\leqslant j\leqslant n}(|a_{ij}|)=a$, $\max_{1\leqslant j\leqslant n}(|q_j-q_j'|)=\sigma_3$, where $a>0$, $\sigma_3>0$. Similarly,

$$\begin{aligned} & |f(t,p_i)-f(t',p_i')| \\ & \leqslant\left(\left|\frac{\omega(\sigma_1+\sigma_2)}{\sigma_1}\right|+|3\mu_iM^2|+\left|\frac{2\mu_iMN^2}{\sigma_1}\right|+\frac{na\sigma_3}{\sigma_1}\right)|p_i-p_i'| \\ & =L_2|p_i-p_i'|, \end{aligned} \tag{11}$$

where $L_2=\left|\frac{\omega(\sigma_1+\sigma_2)}{\sigma_1}\right|+|3\mu_iM^2|+\left|\frac{2\mu_iMN^2}{\sigma_1}\right|+\frac{na\sigma_3}{\sigma_1}$.

From eqs. (9) and (11), it can be ensured that the system in eq. (5) matches the condition of a Lipschitz-type function, i.e., $|f(t,X)-f(t,X')|\leqslant L|X-X'|$, where $L=\max(L_1, L_2)$. Hence, there exists a unique solution for the system in eq. (4) with any initial value (p_{i0}, q_{i0}).

To make the CPG network model (4) more appropriate for engineering applications, the CPG network model is simplified using nearest-neighbor connections as eq. (12).

$$\begin{cases} \dot{p}_i=\omega(p_i-q_i)-\mu_ip_i(p_i^2+q_i^2)+\sum_{j=i-1,i+1}a_{ij}q_j, \\ \dot{q}_i=\omega(p_i+q_i)-\mu_iq_i(p_i^2+q_i^2), \end{cases} \tag{12}$$

where i (i = 1, …, n, n+1) indicates the i-th joint, n represents the joint number of the flexible posterior body, and $i=n+1$ denotes the caudal fin. Let the left pectoral fin be the n+2-th propulsion component in the robotic fish, and the right pectoral fin be the n+3-th propulsion component. In accordance with the coupling between the two pectoral fins and the first body joint, as illustrated in Figure 4, these CPG units constitute an integrated CPG network topology.

2.3 CPG coupling and multimodal swimming

Generally, finding suitable connection weights (i.e., coupling coefficients) between CPG units is of great significance to efficient and stable swimming. On one hand, for identical propulsion components in the robotic fish, the phase-lag of each joint can be derived in terms of the traveling body wave exhibited in steady fish swimming. The coupling coefficients for the multi-joint posterior body are then determined in sequence. Refer to our previous paper [24] for more details on the parameter estimation for CPG coupling. As for flexible pectoral fins, the coupling coefficients between them can employ peer-to-peer relationships. That is, the coupling coefficient $a_{n+2,n+3}$ denoting the impact parameter on the left pectoral fin from the right one is assumed to equal $a_{n+3,n+2}$ indicating the impact parameter on the right pectoral fin from the left one.

On the other hand, for different types of propulsion components, such as diffusive couplings between pectoral fins and body joints, the connection weights are difficult to determine. To guarantee in-phase movements, the coupling coefficient is simply chosen as $a_{n+2,1}=a_{n+3,1}=\omega_{1\max}/\omega_{2\max}$, where $\omega_{1\max}$ is the maximum frequency of the driving motor for pectoral fins, and $\omega_{2\max}$ corresponds to the maximum

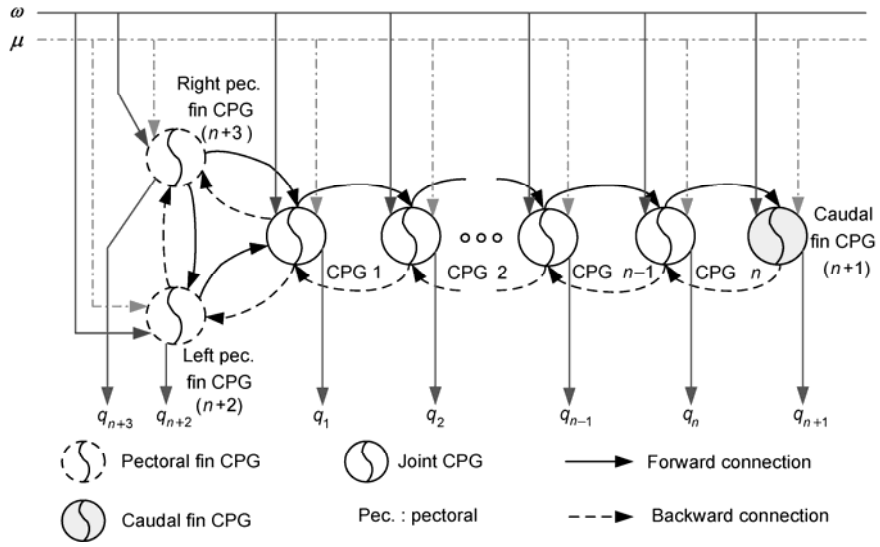

Figure 4 Topology of the formulated CPG network.

frequency of the driving motor for the first joint in the moving posterior body. Thus, all the characteristic parameters connecting the adopted CPGs in eq. (4) can be determined. Table 2 lists the CPG parameters applied to the robotic fish.

With the above CPG parameters, a hybrid amplitude-frequency based approach is applied to CPG-based swimming control. As for the CPG network expressed by eq. (4), it has an intrinsic limit cycle solution, which is a sinusoidal value with an amplitude of $\sqrt{\omega/\mu_i}$ and a period of $2\pi/\omega$. Hence, changing parameters μ_i and ω will alter the oscillatory frequency f simultaneously with the oscillatory amplitude. It should be noted that varying parameter ω will affect the oscillatory amplitude only very slightly, whereas it will change the oscillatory frequency dramatically.

For our robotic fish, forward swimming can be achieved by rhythmic BCF movements and/or by coordinated PF movements, similar to a real fish. In essence, the pectoral fins help control the direction and the movement of a fish. To generate a propulsive force opposite to that of forward motion, an intuitive way is to use the artificial pectoral fins. Compared to swimming forward using the pectoral fins, a pitch bias angle of π is superposed on the output signals in eq. (4), leading to backward propulsion. That is, $q_{ib} = \pi$ (i = 5,6), where q_{ib} indicates the bias associated with the i-th joint. This anti-phase driving also conforms well to the neural control of backward swimming in lamprey [11]. Furthermore, diving motion under a zero speed condition can be attained by setting $q_{ib} \in (0,\pi)$ (i = 5,6). More interestingly, as the robot is independently driven by the pectoral fins, it will dive backward into the water with $q_{ib} \in (\pi/2, \pi)$, whereas it will dive forward into the water with $q_{ib} \in (0, \pi/2)$. Furthermore, the robot enters the ascending mode when $q_{ib} \in (-\pi, 0)$.

Table 2 CPG parameter values applied to the robotic fish

Parameters	Value
a_{ij} (j=i–1, i+1)	$a_{i,i-1} = a_1 = -19.6$, $a_{i,i+1} = a_2 = -19$ (body, i = 1,…,4)
$a_{n+2,n+3}$, $a_{n+3,n+2}$	$a_{n+2,n+3}$=$a_{n+3,n+2}$=2 (pectoral-pectoral)
$a_{n+2,1}$, $a_{n+3,1}$	$a_{n+2,1} = a_{n+3,1}$ = 2.33 (pectoral-body)
μ_i	$\mu_1 = 0.111$, $\mu_2 = 0.049$, $\mu_3 = 0.028$, $\mu_4 = 0.111$ (body)
	$\mu_5 = \mu_6 = 0.111$ (pectoral)
q_{ib}	q_{ib} = 0 (forward BCF)
	$q_{ib} \in (0,\pi)$ (diving, i = 5,6)
	$q_{ib} \in (-\pi,0)$ (ascending, i = 5,6)

Besides rhythmic swimming, discrete turning motions can be generated in several ways. For example, the robot can dynamically change its heading by adding deflections to the moving joints. Another steering method is to generate asymmetrical undulating amplitude in one undulation period. A robotic fish with artificial pectoral fins can perform various lateral turns through asymmetric drive. Actually, the incorporation of a sensory feedback term into the CPG network model in eq. (12) will also trigger turning motions, by forcing some CPG units to stop oscillating. A sensory feedback coupled system can be created as

$$\begin{cases} \dot{p}_i = \omega(p_i - q_i) - \mu_i p_i(p_i^2 + q_i^2) + \sum\limits_{j=i-1,i+1} a_{ij} q_j + s_i, \\ \dot{q}_i = \omega(p_i + q_i) - \mu_i q_i(p_i^2 + q_i^2) - s_i, \end{cases} \tag{13}$$

where s_i (i =1, …, n+3) is the feedback signal related to the i-th CPG unit. A simple example of a feedback signal triggered turn is shown in Figure 5, where ω = 6.28 rad/s. Specifically, an obstacle signal measured by infrared sensors activates the turning mode within the 3–6.2 s interval, accompanied by a feedback term s_1 = 100 input into eq. (13). This causes the first body joint to become saturated and then to stop oscillating, which eventually makes the robot execute a turning motion. After the obstacle information is removed,

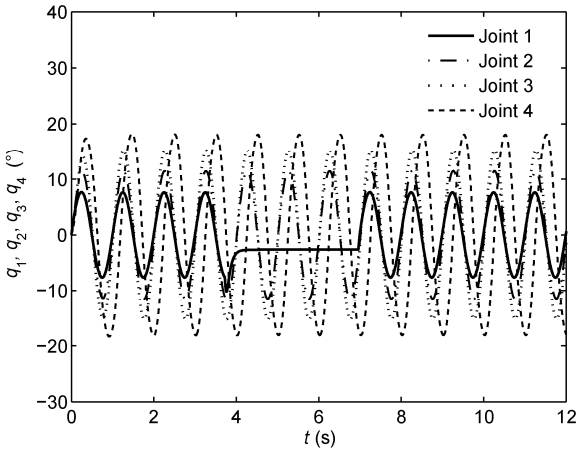

Figure 5 CPG output signals for joints in a switch case between swimming straight and turning movement. Note that q_i is the i-th CPG unit output signal fed into the motor.

the CPGs will regenerate rhythmic forward swimming. Note that the magnitude of the induced turning relies heavily on the value of s_1, which is empirically decided by experiments or by fuzzy logic rules. This example also shows that smooth switching between different modes triggered by the sensory feedback might be feasible. This interesting topic will be addressed in another paper in the near future.

3 Experiments and results

To evaluate the proposed CPG-based swimming control method, extensive experiments have been carried out in a lake and swimming tank. The swimming performance of the robotic fish is evaluated by an additional vision measuring system, mainly involving color-based adaptive segmentation and a closure operation [25]. As illustrated in Figure 6, the robotic fish can perform multiple swimming modes successfully.

3.1 Experiments

The first experiment set out to explore the effects of changing μ_i in the CPG network model according to the velocity. In Figure 7, three parameter sets in the BCF mode are compared, where parameter 1 = {μ_1=0.25, μ_2=0.125, μ_3=0.067, μ_4=0.05}, parameter 2 = {μ_1=0.125, μ_2=0.063, μ_3=0.033, μ_4=0.025}, and parameter 3 = {μ_1=0.063, μ_2=0.031, μ_3=0.017, μ_4=0.013}. It is clear that the final propulsive velocity increases with a decreasing μ_i, but with an increasing f. Recalling that the amplitude of the limit cycle solution attached to eq. (4) is $\sqrt{\omega/\mu_i}$, we can easily deduce that a greater swimming amplitude will result in higher speed, agreeing well with biological observations.

In the second experiment, taking into account the smoothness of the CPG governed swimming, we altered the number of joints participating in the fishlike motion. Figure 8

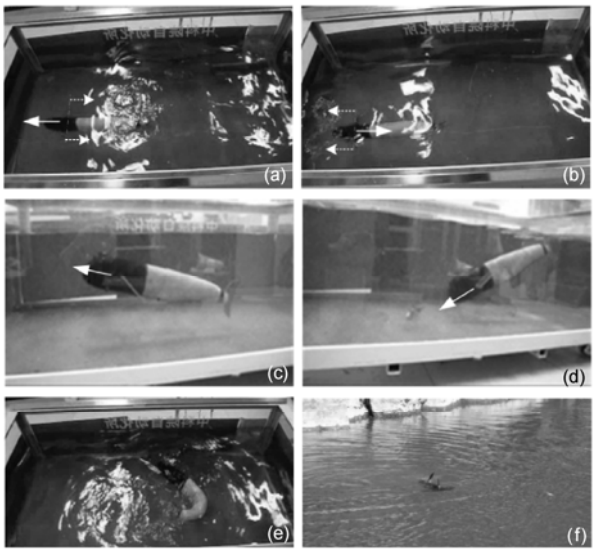

Figure 6 Snapshots of multimodal swimming involving: (a) forward swimming, (b) backward swimming, (c) ascending, (d) diving, (e) coordinated turning, and (f) a field cruise in the lake. Notice that the solid arrow in the figures denotes the propulsion direction of the robotic fish, while the dotted arrow indicates the oscillation direction of the pectoral fins.

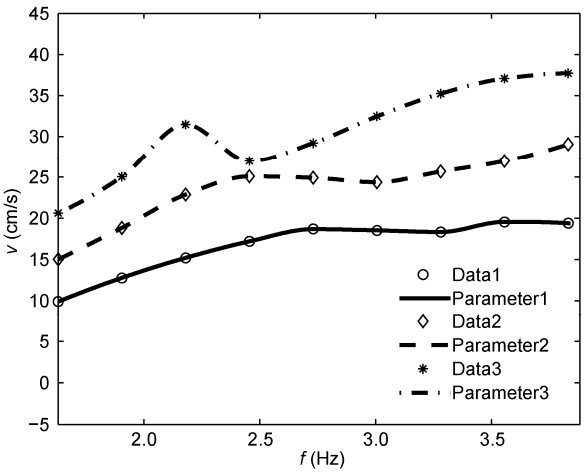

Figure 7 Velocities of BCF-type swimming with varying μ_i and f.

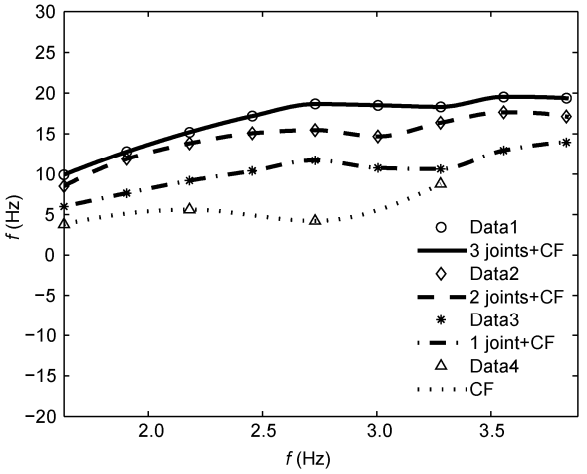

Figure 8 Velocity comparison of four propulsion cases with different joint numbers.

shows four propulsion cases, in which the value of μ_i corresponds to parameter 1. As can be observed, the resulting velocity increases with an increasing number of joints, revealing the power of coordinated propulsion among multiple control surfaces. These two experiments verify the sensitivity of the extracted characteristic parameters, μ_i and ω (=$2\pi f$), facilitating practical application.

Finally, the proposed CPG network model (termed the CPG-based method) was further evaluated against the sine-based body wave fitting method (termed the fish body wave method) in [3]. During BCF-type straight swimming, the acquired yaw, pitch, and roll angles (in a world reference frame) from the fish body wave method were compared with those acquired from the CPG-based method as shown in Figure 9. Here three angle values were measured by MicroStrain's gyro enhanced product, 3DM-GX1. To examine the swimming stability, the amplitude of the robotic fish was abruptly increased at 7 s by changing ω, whereas the amplitude rose continuously after 12 s. Notice that the same parameter variation was applied to the comparative experiments. As can be seen, the CPG-based method achieved a relatively better performance compared to the fish body wave method, particularly with lower pitch and roll angles even in parameter-varying cases. This comparison verifies that the CPG-based method exhibits better dynamic invariability to preserve rhythm because of the limit-cycle characteristics of the CPGs.

3.2 Discussion

As a class of bio-inspired neural networks, CPGs are capable of autonomous, stable, self-modulatory control, constituting an ideal candidate for practical engineering solutions. Although the set of nearest-neighbor-coupled neural oscillators has successfully generated outputs for various swimming modes of a multi-articulated robotic fish in this paper, the underlying CPG coordination mechanisms have not yet been fully unraveled and understood. It is not clear to what extent such CPG coupling and coordination will benefit the high efficiency and striking maneuverability of the fish. Thus, investigating CPG coupling (unidirectional or bidirectional, excitatory or inhibitory) and coordination control thoroughly in the context of bio-inspired robotics is of paramount importance. Additionally, we remark that the limitations of vision-based experimental fields and the lack of sufficient onboard sensors in our demonstration experients have, to some extent, weakened the attainable swimming performance of the developed robot.

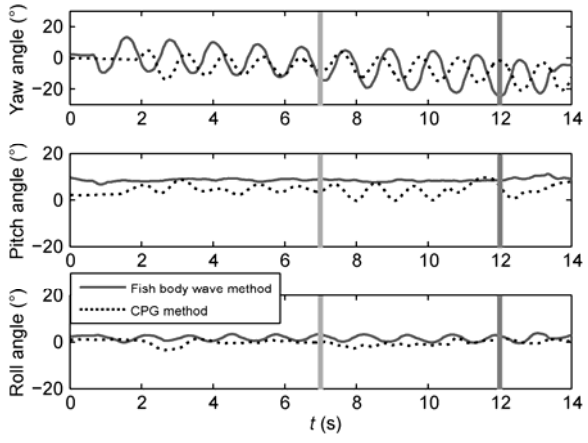

Figure 9 Comparison of the fish body wave method and the CPG-based method for BCF swimming.

4 Conclusion and future work

A CPG network model created by coupling a set of nonlinear neural oscillators has been presented with nearest-neighbor-coupled connections, which can output rhythmic, multimodal swimming. A parameter sensitivity analysis and stability proof for the CPG network has been conducted theoretically. Both numerical analysis and aquatic experiments have primarily verified the effectiveness of the formulated model in generating multimodal swimming. In contrast to the conventional body wave method, the CPG-based method has an enhanced ability to cope with transient transitions and perturbations.

Our future work will focus on thoroughly investigating CPG coupling and the coordination control of CPGs using the fish-inspired robotic testbed. Improving our mechanical design and adding more sensors to endow the robotic fish with more flexibility and adaptability is another ongoing endeavor. Hopefully, designing sensory feedback circuits or further integrating the CPG-based controller into one chip will greatly reduce the system operating time and improve the overall performance.

This work was supported by the National Natural Science Foundation of China (*60775053, 61075102*) *and in part by the Beijing Natural Science Foundation* (*4102063, 4122084*)

1 Triantafyllou M S, Techet A H, Hover F S. Review of experimental work in biomimetic foils. IEEE J Ocean Eng, 2004, 29: 585–594
2 Bandyopadhyay P R. Trends in biorobotic autonomous undersea vehicles. IEEE J Ocean Eng, 2005, 30: 109–139
3 Yu J Z, Tan M, Wang S, et al. Development of a biomimetic robotic fish and its control algorithm. IEEE Trans Syst Man Cybern B, 2004, 34: 1798–1810
4 Liu J D, Hu H S. Biological inspiration: From carangiform fish to multi-joint robotic fish. J Bionic Eng, 2010, 7: 35–48
5 Liang J H, Wang T M, Wen L. Development of a two-joint robotic fish for real-world exploration. J Field Robot, 2011, 28: 70–79
6 Hu T J, Shen L C, Low K H. Bionic asymmetry: From amiiform fish to undulating robotic fins. Chin Sci Bull, 2009, 54: 562–568
7 Ha N S, Goo N S, Yoon H J. Development of a propulsion system for a biomimetic thruster. Chin Sci Bull, 2011, 56: 432–438
8 Barrett D S. Propulsive efficiency of a flexible hull underwater vehicle. Dissertation for Doctoral Degree. Cambridge, MA: Massachusetts Institute of Technology, 1996
9 Kato N. Control performance in horizontal plane of a fish robot with mechanical pectoral fins. IEEE J Ocean Eng, 2000, 25: 121–129

10 Terada Y, Yamamoto I. An animatronic system including lifelike robotic fish. Proc IEEE, 2004, 92: 1814–1820
11 Grillner S, Kozlov A, Dario P, et al. Modeling a vertebrate motor system: Pattern generation, steering and control of body orientation. Prog Brain Res, 2007, 165: 221–234
12 Ijspeert A J. Central pattern generators for locomotion control in animals and robots: A review. Neural Netw, 2008, 21: 642–653
13 Zhou C L, Low K H. Kinematic modeling framework for biomimetic undulatory fin motion based on coupled nonlinear oscillators. In: Proc IEEE/RSJ Int Conf Intell Robot Syst, Taipei, Taiwan, Oct 2010. 34–939
14 Wu X D, Ma S G. Adaptive creeping locomotion of a CPG-controlled snake-like robot to environment change. Auton Robot, 2010, 28: 283–294
15 Wu X D, Ma S G. CPG-based control of serpentine locomotion of a snake-like robot. Mechatronics, 2010, 20: 326–334
16 Wu X D, Ma S G. Sensor-driven neural controller for self-adaptive collision-free behavior of a snake-like robot. In: Proc IEEE Int Conf Robot Autom, Shanghai, China, 2011. 191–196
17 Cohen A H, Holmes P J, Rand R H. The nature of the coupling between segmental oscillators of the lamprey spinal generator for locomotion: A mathematical model. J Math Bio, 1982, 13: 345–369
18 Crespi A, Lachat D, Pasquier A, et al. Controlling swimming and crawling in a fish robot using a central pattern generator. Auton Robot, 2008, 25: 3–13
19 Zhao W, Yu J Z, Fang Y M, et al. Development of multi-mode biomimetic robotic fish based on central pattern generator. In: Proc IEEE/RSJ Int Conf Intell Robot Syst, Beijing, China, 2006. 3891–3896
20 Zhang D B, Hu D W, Shen L C, et al. Design of an artificial bionic neural network to control fish-robot's locomotion. Neurocomputing, 2008, 71: 648–654
21 Degallier S, Ijspeert A J. Modeling discrete and rhythmic movements through motor primitives: A review. Biol Cybern, 2010, 103: 319–338
22 Yu J Z, Wang L, Zhao W, et al. Optimal design and motion control of biomimetic robotic fish. Sci China Ser F - Inf Sci, 2008, 51: 535–549
23 Zhang D G, Zhu K Y. Computer simulation study on central pattern generator: From biology to engineering. Int J Neural Syst, 2006, 16: 405–422
24 Wang M, Yu J Z, Tan M. Parameter design for a Central Pattern Generator based locomotion controller. In: Proc 1st Int Conf Intell Robot Appl, Part I, LNAI 5314, Wuhan, China, Oct 2008. 352–361
25 Yu J Z, Fang Y M, Wang L, et al. Visual tracking of multiple robotic fish for cooperative control. In: Proc IEEE Int Conf Robot Biomim, Kunming, China, Dec 2006. 85–90